

Report Number 11/19

**A perturbation analysis of spontaneous action potential initiation
by stochastic ion channels**

by

James P. Keener and Jay M. Newby



Oxford Centre for Collaborative Applied Mathematics
Mathematical Institute
24 - 29 St Giles'
Oxford
OX1 3LB
England

A perturbation analysis of spontaneous action potential initiation by stochastic ion channels

James P. Keener¹ and Jay M. Newby²

¹*Department of Mathematics, University of Utah, 155 South 1400 East, Salt Lake City UT 84112*

²*Mathematical Institute, University of Oxford, 24-29 St. Giles', Oxford, OX1 3LB, UK*

A stochastic interpretation of spontaneous action potential initiation is developed for the Morris-Lecar equations. Initiation of a spontaneous action potential can be interpreted as the escape from one of the wells of a double well potential, and we develop an asymptotic approximation of the mean exit time using a recently-developed quasi-stationary perturbation method. Using the fact that the activating ionic channel's random openings and closings are fast relative to other processes, we derive an accurate estimate for the mean time to fire an action potential (MFT), which is valid for a below-threshold applied current. Previous studies have found that for above-threshold applied current, where there is only a single stable fixed point, a diffusion approximation can be used. We also explore why different diffusion approximation techniques fail to estimate the MFT.

I. INTRODUCTION

Stochasticity plays an important role in many electrophysiological contexts. The onset of pathological dynamical behaviors such as epilepsy and cardiac fibrillation are most likely the result of random fluctuations that move an otherwise deterministic dynamical system from one basin of attraction to another. For example, spontaneous release of calcium from the sarcoplasmic reticulum of cardiac cells is thought to be related to delayed afterdepolarizations (DAD's), which are in turn believed to initiate fatal cardiac arrhythmias [1, 2]. Stochastic opening and closing of high-conductance K-Ca channels is thought to be responsible for the highly stochastic bursting patterns of isolated pancreatic beta cells [3].

The Hodgkin-Huxley equations have been used successfully to describe many important features of the behavior of nerve cells. These equations, like most conductance-based ionic models, calculate average ionic currents using channel open probabilities. Although the expectation is that because of the law of large numbers, average channel behavior gives adequate accuracy in many situations, there are several questions that cannot be answered by averaged equations. For example, how often can an action potential be initiated spontaneously, i.e., without external stimulus? How big is big, that is, at what channel density can stochastic effects be ignored? Said another way, how fast do stochastic equations of action potential dynamics converge to their deterministic limit? What are the effects of stochastic behavior on the stimulus threshold?

To answer these questions we must examine the role of stochastic ion channel openings and closings on the initiation of an action potential. While this paper focuses on the Morris-Lecar equations, the general problem can be described as follows. Suppose the initial (upstroke) dynamics of an action potential are described by a deterministic bistable equation, say

$$\frac{dv}{dt} = -I_{\text{ion}}(v) + I(t), \quad (1.1)$$

where v is the transmembrane potential, $I(t)$ is the applied stimulus current, and $I_{\text{ion}}(v)$ represents the ionic currents and has three zeros, the smallest of which corresponds to the stable resting potential, and the largest of which corresponds to the excited state. Past studies have proposed a stochastic differential equation (SDE) version of (1.1), where the influence of stochastic ion channels is modeled as a white noise [4]. This interpretation replaces the deterministic model with a Langevin equation of the form

$$dV = (-I_{\text{ion}}(V) + I(t))dt + \sigma(V) * dW, \quad (1.2)$$

where $W(t)$ is the standard Wiener process and σ is the noise amplitude. Note that we use the symbol $*$ to signify that the SDE is to be interpreted in the sense of Stratonovich. This equation is paired with the Fokker-Planck (FP) equation for the probability density for the random variable $V(t)$, which is a linear, second-order parabolic PDE. In this context, if the applied current is below the deterministic threshold, the bistable function $I_{\text{ion}}(v)$ is viewed as the derivative of a double well potential, and initiation of a spontaneous action potential is viewed as the escape from the lower well to the upper well. On the other hand, if the applied current is above threshold, the minimum of the lower well vanishes, and initiation of an action potential is simply the mean time to reach the upper well. In either case, one can formulate the mean firing time (MFT) as a mean first passage time problem [5]. However, before using a Langevin description, one must determine the amplitude of the noise $\sigma(V)$ by careful consideration of the underlying kinetics of the ion channels.

Channel noise arises from stochastic opening and closing of ion channels (see [6] for a review). A more realistic stochastic version of (1.1) would account for the discrete opening and closing events of the ion channels [4, 7–10]. This hybrid continuous/discrete process is given by

$$\dot{V} = -I_{\text{ion}}(V, S) + I(t), \quad (1.3)$$

where $S(t)$ describes the state of the population of ion channels, and $I_{\text{ion}}(V, S)$ is the state-dependent ionic cur-

rent. For example, suppose we have N independent channels that can either be open or closed, with transitions between these two states described by the two-state Markov process

$$C \xrightleftharpoons[\beta]{\alpha} O \quad (1.4)$$

where the transition rates α and β are dependent on v . Since there are N such channels, the overall state diagram is

$$S_0 \xrightleftharpoons[\beta]{N\alpha} S_1 \xrightleftharpoons[2\beta]{(N-1)\alpha} S_2 \cdots S_{N-1} \xrightleftharpoons[N\beta]{\alpha} S_N \quad (1.5)$$

where in state S_n there are n open channels. Notice that this random process is discrete, whereas the Langevin equation (1.2) assumes that the channel noise is continuous. Just as the Langevin equation is paired with a FP equation, the coupled random processes $V(t)$ and $S(t)$ are described by the probability density function $\text{Prob}\{V(t) \in (v, v + dv), S(t) = n\} = P(v, n, t)dv$, which satisfies a differential Chapman-Kolmogorov (CK) equation [5].

Using perturbation methods, one can reduce the CK equation to a FP equation, which is a consistent and accurate means of deriving a Langevin description of the stochastic process. Collectively, these reductions are known as diffusion approximations. There are a variety of methods to derive diffusion approximations, divided into two main categories: quasi-steady-state (QSS) methods that derive an equation for the marginal distribution $u(v, t) = \sum_n p(v, n, t)$ and system size expansion methods that replace the discrete noise with a continuous noise by treating $s = n/N$ as a continuous state. Each of these formulations converge to the deterministic equation (1.1) in the appropriate limit, that is, in the thermodynamic limit $N \rightarrow \infty$ and in the limit of fast channel switching. The QSS methods exploit the fact that channels switch between their open and closed states quickly compared to changes in voltage, and results in the greatest reduction of complexity; the corresponding Langevin equation has the form (1.2). The system-size expansion approach can be applied to more complicated ion channel models, such as the Hodgkin-Huxley model, and in the case of Morris-Lecar dynamics the approach results in two coupled SDEs

$$\dot{V} = -I_{\text{ion}}(V, S) + I(t), \quad (1.6)$$

$$dS = \frac{1}{\tau(V)} (S_{\infty}(V) - S) dt + \sigma(V) dW. \quad (1.7)$$

Several previous studies have developed diffusion approximations for the Hodgkin-Huxley model [4, 9, 11–13], which use either the system-size expansion to obtain a system of coupled SDEs like (1.6) or both methods in succession to obtain a single SDE like (1.2). In either case, the goal is to reduce a discrete stochastic process to an effective continuous process.

All of these approaches work well to approximate the MFT if the applied current is above threshold and the underlying deterministic system has only one stable fixed point. However, for the case where the applied current is below threshold and the deterministic system is bistable, the approximations for the MFT have exponentially large errors. As we show in this paper, both the QSS and system-size expansion methods break down in this case for the same reasons. This breakdown is indicative of large deviation behavior and is closely related to the failure of asymptotic methods to resolve exponentially-small terms [14–21].

In this paper we resolve the inaccuracy of previous analytical- and simulation-based approximations of the MFT when the stimulus current is below threshold. We derive an accurate analytical approximation based on methods developed previously for a model of molecular motor transport [22, 23]. To explore the mathematical issues involved, we also develop and compare diffusion approximations based on QSS and system-size expansion methods. Our results suggest that neurons are far more responsive to subthreshold stimuli than predicted by stochastic models that use a continuous approximation for the channel noise.

The organization of the paper is as follows. First, in Section II we develop the stochastic Morris-Lecar model and derive the CK equation for its probability density function. For below-threshold stimuli, we derive a quasi-stationary approximation of the MFT in Section III. Then, in Section IV we use the QSS analysis to reduce the CK equation to an effective FP equation and compute the MFT for a spontaneous action potential, which disagrees with the quasi-stationary approximation by several orders of magnitude. To fully explore the issues involved in the breakdown of different diffusion approximations, we also apply the system-size expansion to the model in Section V to obtain a two-dimensional FP equation. We then apply a QSS analysis to further reduce the FP equation to one dimension and show that the result is identical to that obtained from the QSS analysis of the full model, which means that for above-threshold stimulus both diffusion approximation techniques are consistent. However, we also apply the quasi-stationary analysis to the result of the system-size expansion and find the MFT exhibit the same errors as the QSS diffusion approximation. We conclude that for spontaneous action potential generation, the fully discrete channel noise model must be used to obtain an accurate estimate of the MFT. Finally, in Section VI results are illustrated with strength-duration curves and firing probabilities after a stimulus of fixed duration.

II. THE STOCHASTIC MORRIS-LECAR MODEL

The Morris-Lecar equations are

$$C_m \frac{dv}{dt} = g_{Na} m_\infty(v)(v_{Na} - v) + g_K w(v)(v_K - v) + g_L(v_L - v) + I(t), \quad (2.1)$$

$$\frac{dw}{dt} = \frac{\phi}{\tau}(w_\infty(v) - w), \quad (2.2)$$

where

$$m_\infty(v) = 0.5 \left(1 + \tanh \left(\frac{v - v_1}{v_2} \right) \right), \quad (2.3)$$

$$w_\infty(v) = 0.5 \left(1 + \tanh \left(\frac{v - v_3}{v_4} \right) \right), \quad (2.4)$$

$$\tau^{-1} = \cosh \left(\frac{v - v_3}{2v_4} \right). \quad (2.5)$$

Parameter values are specified in Table I. Because our goal is to study action potential initiation, we set the slow variable w to its initial value $w(0) = 0.27$. This is a standard method for studying deterministic action potential initiation, and a key assumption in our stochastic model is that because w is a slow variable, any fluctuations in the Sodium channel conductance will have a small effect on the value of w until the voltage increases past threshold. Once this happens, the slow dynamics of w reset the system back to the resting voltage. For simplicity, we also assume a constant stimulus current $I(t) \equiv I > 0$. We can then reduce equations (2.1) to

$$C_m \frac{dv}{dt} = m_\infty(v)f(v) - g(v), \quad (2.6)$$

where $f(v) = g_{Na}(v_{Na} - v)$ represents the gated (i.e. Sodium) current, $g(v) = -g_{eff}(v_{eff} - v) - I$ represents ungated currents, and

$$v_{eff} = \frac{g_K w(0)v_K + g_L v_L}{g_K w(0) + g_L}, \quad g_{eff} = g_K w(0) + g_L. \quad (2.7)$$

$v_{Na} = 120\text{mV}$	$g_{Na} = 4.4\text{mS/cm}^2$
$v_K = -84\text{mV}$	$g_K = 8\text{mS/cm}^2$
$v_L = -60\text{mV}$	$g_L = 2\text{mS/cm}^2$
$v_{eff} = -62.3\text{mV}$	$g_{eff} = 2.2\text{mS/cm}^2$
$v_1 = -1.2\text{mV}$	$v_2 = 18\text{mV}$
$v_3 = 2\text{mV}$	$v_4 = 30\text{mV}$
$C_m = 20\mu\text{F/cm}^2$	$\phi = 0.04\text{ms}^{-1}$

TABLE I. Parameter values for the Morris-Lecar equations [24].

Note that $g_{Na} > g_{eff}$. We now introduce the SDE for the random variable $V(t)$ given by

$$\dot{V} = \frac{1}{N} \sum X_i(t) f(V) - g(V), \quad (2.8)$$

where each of the random variables $X_i(t)$ is either zero or one, depending on whether the i^{th} ionic channel is closed (0) or open (1). Individual channels are taken to be independent; they transition to the open state at the rate $\alpha(v)$ and to the closed state at the voltage-independent rate β . The transition rates are chosen so that the steady state fraction of open channels, $a(v)$, satisfies

$$a(v) \equiv \frac{\alpha(v)}{\alpha(v) + \beta} = m_\infty(v), \quad (2.9)$$

which is true if

$$\alpha(v) = \beta \exp \left[\frac{2}{v_2} (v - v_1) \right]. \quad (2.10)$$

It follows that the random variable $S(t) = \sum X_i(t)$ is determined by a birth/death process, with a finite number of states; that is, $S \in \{0, 1, \dots, N\}$. The transitions between each state are given by (1.5).

The differential Chapman-Kolmogorov (CK) equation for the probability density function $p(v, n, t | v_0, n_0, 0) dv \equiv \text{Prob}\{V(t) \in (v, v + dv), S(t) = n | V(0) = v_0, S(0) = n_0\}$ is

$$\begin{aligned} \frac{\partial p}{\partial t} = & -\frac{\partial}{\partial v} \left(\left(\frac{n}{N} f(v) - g(v) \right) p \right) \\ & + (N - n + 1) \alpha(v) p(v, n - 1, t) \\ & - ((N - n) \alpha(v) + n \beta) p(v, n, t) \\ & + (n + 1) \beta p(v, n + 1, t), \end{aligned} \quad (2.11)$$

for $n = 0, 1, \dots, N$. The initial condition is

$$p(v, n, 0) = \delta(v - v_0) \delta_{n, n_0}. \quad (2.12)$$

Because the RHS of (2.8) is negative for large V and positive for small V , there is an interval to which the voltage is confined. Define v_a to be that value of v for which $\dot{V} = 0$ when there are no open channels ($n = 0$), i.e., $g(v_a) = 0$, and define v_b to be that value of v for which $\dot{V} = 0$ with all the channels open ($n = N$), i.e., $f(v_b) - g(v_b) = 0$. Then, since $v_{eff} < v_{Na}$, if $V < v_a$ ($V > v_b$) then $\dot{V} > 0$ ($\dot{V} < 0$) for all $n = 0, \dots, N$. Thus, once the voltage is in the interval (v_a, v_b) , where

$$v_a = v_{eff} - \frac{I}{g_{eff}}, \quad v_b = \frac{I + g_{Na} v_{Na} - g_{eff} v_{eff}}{g_{Na} - g_{eff}}, \quad (2.13)$$

the voltage remains in this interval for all time. Furthermore, $p(v, t) \rightarrow 0$ as $t \rightarrow \infty$ for all v outside this interval, and if $p(v, 0) = \delta(v - v_0)$, with $v_0 \in (v_a, v_b)$, then $p(v, t) = 0$ for all $v \in (-\infty, v_a] \cup [v_b, \infty)$ and $t \geq 0$.

Nondimensionalize the equations with the rescaling

$$v \rightarrow \frac{v - v_{eff}}{\Gamma}, \quad I \rightarrow \frac{I}{\Gamma g_{eff}}, \quad t \rightarrow \frac{t g_{eff}}{C_m}, \quad (2.14)$$

where

$$\Gamma = \frac{g_{\text{Na}}v_{\text{Na}} - g_{\text{eff}}v_{\text{eff}}}{g_{\text{Na}} - g_{\text{eff}}} - v_{\text{eff}}. \quad (2.15)$$

The voltage Γ is positive provided that

$$v_{\text{Na}} - v_{\text{eff}} > \frac{g_{\text{Na}} - g_{\text{eff}}}{g_{\text{Na}}}. \quad (2.16)$$

Then, the interval $(v_a, v_b) \rightarrow (\vartheta_a, \vartheta_b)$ where

$$\vartheta_a = -I, \quad \vartheta_b = 1 + \frac{I}{g_{\text{Na}}/g_{\text{eff}} - 1}. \quad (2.17)$$

Finally, we define the nondimensional voltage threshold to be

$$\vartheta_1 = (v_1 - v_{\text{eff}})/\Gamma. \quad (2.18)$$

It is convenient to rewrite the above CK equation in matrix form by defining the probability vector $\mathbf{p}(v, t)$, having entries $p_n(v, t) = p(v, n, t)$. We define the tridiagonal matrix $A(v)$ to be the transition-rate matrix for the Markov process, with entries

$$\begin{aligned} A_{n,n-1} &= (N - n + 1)\alpha, & A_{n,n} &= -(N - n)\alpha - n\beta, \\ A_{n,n+1} &= (n + 1)\beta, \end{aligned} \quad (2.19)$$

for $n = 0, 1, \dots, N$. We also define the diagonal matrix $F(v)$ and the vector $\mathbf{f}(v)$ as having entries

$$F_{n,n} = \mathbf{f}_n = \frac{n}{N}f(v) - g(v), \quad n = 0, 1, \dots, N. \quad (2.20)$$

The vector \mathbf{f} represents the total current as a function of the number of open channels n . Note that for notational convenience, the explicit dependence of vectors and matrices on the voltage v may be suppressed.

If the transitions between discrete states are fast compared to the time scale of change of v , then the elements of A are typically much larger than the elements of F . This difference in time scale can be emphasized by rescaling the matrix A by the dimensionless parameter $\epsilon = g_{\text{eff}}/(C_m\beta)$ the ratio of typical time scales, which we assume to be small, with $\epsilon A \rightarrow A$. The rescaled transition rates are now $\beta = 1$ and

$$\alpha(v) = \exp[\theta_1 v - \theta_2], \quad (2.21)$$

with the nondimensional parameters

$$\theta_1 = \frac{2\Gamma}{v_2}, \quad \theta_2 = 2 \left(\frac{v_{\text{eff}} - v_1}{v_2} \right). \quad (2.22)$$

Our goal is to take advantage of this time scale difference to approximate the average time to a spontaneous action potential. The CK equation (2.11) can now be written as

$$\frac{\partial \mathbf{p}}{\partial t} = -\frac{\partial}{\partial v}(F\mathbf{p}) + \frac{1}{\epsilon}A\mathbf{p}. \quad (2.23)$$

Since A is a transition matrix, it must be that its column sums are zero, and all its nonzero eigenvalues are negative. It follows that A has a zero eigenvalue with a positive right eigenvector $\boldsymbol{\rho}$ and left eigenvector $\mathbf{1}$ with entries $\mathbf{1}_n = 1$. We normalize $\boldsymbol{\rho}$ so that $\mathbf{1}^T \boldsymbol{\rho} = 1$. In our case, we can determine the nullvector explicitly. We find that $\boldsymbol{\rho}$ is the vector with components

$$\rho_n = \binom{N}{n} a(v)^n b(v)^{N-n}, \quad (2.24)$$

where $a(v)$ is defined above in (2.9) and $b(v) = 1 - a(v)$. Notice that $\boldsymbol{\rho}$ is a positive vector that is normalized to sum to one, which means that it is a discrete probability distribution. Indeed, the distribution function for the voltage-clamped process (i.e. the discrete process with v fixed) evolves to $\boldsymbol{\rho}$ in the limit $t \rightarrow \infty$, and we refer to $\boldsymbol{\rho}$ as the steady-state distribution. One can immediately define the mean of the vector \mathbf{f} with respect to this distribution as

$$\nu(v) \equiv \mathbf{f}^T \boldsymbol{\rho} = a(v)f(v) - g(v), \quad (2.25)$$

which is the deterministic limit of the total current and plays an important role throughout the analysis in this paper.

The key quantity that we wish to estimate with this model is the mean time to fire an action potential (MFT) as a function of the stimulus current; that is, the average time for the voltage to evolve from its resting potential v_0 (at zero applied current) to the deterministic voltage threshold v_1 .

In Fig. 1a, the antiderivative of the RHS of (2.6) with respect to v is plotted for different values of constant stimulus current I . This curve can be interpreted as an effective stability landscape, and the minima and maxima correspond to fixed points. For $I < I_*$, there are three fixed points, consisting of two stable fixed points (minima) separated by an unstable saddle point (maximum). The stable fixed point to the left of the saddle corresponds to the stable resting state, and the stable fixed point to the right corresponds to the excited state. As $I \rightarrow I_*$ there is a saddle-node bifurcation, and the stable resting state vanishes. Once the voltage reaches the excited state, the slow w dynamics from the Potassium channels return the system to the resting voltage.

In the deterministic model, the stimulus current must exceed the deterministic threshold I_* before an action potential can be initiated, and the MFT is infinite for $I < I_*$, but for the stochastic model this time is finite for all values of stimulus current. Thus, there is a qualitative difference in the MFT depending on whether $I < I_*$ or $I > I_*$. In the former case, fluctuations in the states of the ion channels must push the voltage away from the stable resting fixed point to the unstable fixed point, which is much like escape of a diffusing particle from the left to the right well in a double well potential—a classical problem in physics. In the latter case, there is no stable

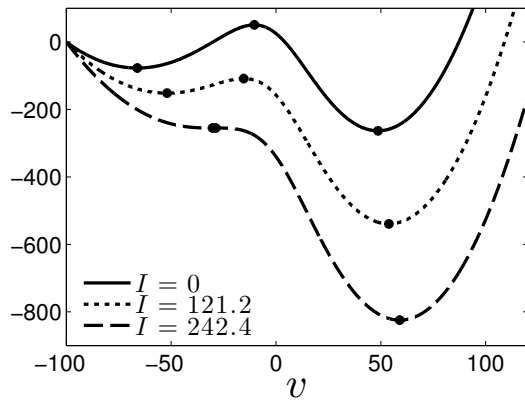


FIG. 1. Deterministic fast dynamics of the Morris-Lecar model (2.6). a) the double-well potential obtained from integrating $a(v)f(v) - g(v)$ (the RHS of (2.6)) over v for different values of stimulus current I . b) The functions $a(v)f(v)$ (grey line) and $g(v)$ (black lines) which have intersections corresponding to the deterministic fixed points.

resting fixed point, and the channel noise causes the firing time to fluctuate about the deterministic limit. Each case requires a different analysis to accurately approximate the MFT.

III. QUASI-STATIONARY APPROXIMATION

To approximate the mean time to fire an action potential for the case where $I < I_*$, we use a quasi-stationary approximation. The stability landscape (see Fig. 1a) contains two wells corresponding to the two stable fixed points of the system. The process begins in the left well at the stable resting voltage, v_0 , and on short time scales the solution rapidly converges to the stationary distribution that sees only the left well; that is, all probability is contained in the left well. Then, on a longer time scale probability slowly leaks into the right well until the full stationary solution is reached. To estimate the time scale of transition from the left to the right well, we place an absorbing boundary at the unstable fixed point, v_* , instead of v_1 , because the time to reach v_1 once v_* is reached is insignificant compared to the time to reach v_* from the stable fixed point v_0 . Note that v_0 depends on the applied current, and we assume that the process starts at the resting voltage with no applied current. However, as is shown in this section, there is little distinction between different starting positions inside the well, and the initial conditions can be chosen from the stationary distribution of the left well.

Let T be the random variable equal to the time at which the particle reaches v_* for the first time, given that it started at v_0 . Our goal is to approximate the probability density for T , which is related to the solution of (2.23) combined with the absorbing boundary condition

$$p_n(v_*, t) = 0, \quad \text{for } n = 0, \dots, k-1, \quad (3.1)$$

where $0 < k < N$ is the number of negative components of \mathbf{f} at the boundary satisfying $Na(v_*) < k < Na(v_*) + 1$, so that

$$k = \text{ceil}(Na(v_*)). \quad (3.2)$$

Recall that the elements of the vector \mathbf{f} are increasing with n , and that there is always at least one negative component for all $v \in (\vartheta_a, \vartheta_b)$ (see (2.13)).

To see how the addition of the absorbing boundary sets up the first exit time problem, define the survival probability

$$\mathcal{S}(t) \equiv \sum_{n=0}^N \int_{\vartheta_a}^{v_*} p_n(v, t) dv \quad (3.3)$$

to be the probability the voltage has not yet reached the absorbing barrier at time t . By integrating (2.23) over the domain (ϑ_a, v_*) and summing over the discrete states we find that

$$\frac{d\mathcal{S}}{dt} = -\mathbf{f}^T \mathbf{p}(v_*, t), \quad (3.4)$$

where we have used the fact that $\mathbf{p}(v, t) \rightarrow 0$ as $v \rightarrow \vartheta_a$. The distribution function for the first-passage time T is $\text{Prob}\{t > T\} = -\mathcal{S}(t)$, and the corresponding density function is given by $\mathcal{F}(t) \equiv -\frac{\partial \mathcal{S}}{\partial t}$. It is useful to interpret the density function for T as the probability flux at the absorbing boundary, which is defined by $\mathcal{J} \equiv \mathbf{f}^T \mathbf{p}$ and satisfies

$$\sum_{n=0}^N \frac{\partial p_n}{\partial t} = -\frac{\partial \mathcal{J}}{\partial v}. \quad (3.5)$$

We can approximate this flux using a spectral projection method [18]. Consider an eigenfunction expansion of the time-dependent solution

$$\mathbf{p}(v, t) = \sum_{j=0}^{\infty} c_j e^{-\lambda_j t} \phi_j(v), \quad (3.6)$$

where the eigenfunctions satisfy the equation

$$L\phi_j \equiv \frac{d}{dv}(F\phi_j) - \frac{1}{\epsilon}A\phi_j = \lambda_j \phi_j \quad (3.7)$$

and the boundary condition

$$(\phi_j)_n(v_*) = 0, \quad \text{for } n = 0, \dots, k-1. \quad (3.8)$$

The presence of an absorbing boundary has two important implications for the eigenfunction expansion (3.6). First, we note that if we replace the absorbing boundary by a reflecting boundary then the principle eigenvalue is $\lambda_0 = 0$, which means that after appropriate normalization, the eigenfunction ϕ_0 is the stationary density. With the absorbing boundary, the principal eigenvalue is exponentially small compared to the remaining eigenvalues. That is, $\lambda_0 = \mathcal{O}(e^{-C/\epsilon})$ for some $C > 0$, and

$C_j = \mathcal{O}(1)$, $j = 1, 2, \dots$, which means that all other eigenmodes decay to zero much faster than the perturbed stationary density. Because of the assumed separation of timescales, we can estimate the long-time behavior of the solution with

$$\mathbf{p}(v, t) \sim \phi_0(v) e^{-\lambda_0 t}. \quad (3.9)$$

With the approximation (3.9), it follows from (3.4) that the first exit time density is

$$\mathcal{F}(t) \sim \lambda_0 e^{-\lambda_0 t}, \quad \lambda_1 t \gg 1, \quad (3.10)$$

so that the density function is asymptotically exponential. Furthermore, the mean exit time is simply given by

$$T_1 \sim \frac{1}{\lambda_0}, \quad (3.11)$$

so that the eigenvalue λ_0 is the approximate firing rate of the neuron. Our goal is then to compute an approximation for the principle eigenvalue λ_0 and the eigenfunction ϕ_0 , satisfying (3.7).

A. Eigenfunction approximation

We begin by using the WKB method [14] to compute an approximation, $\phi_\epsilon \sim \phi_0$ that does *not* satisfy the absorbing boundary condition. That is, we seek an approximate solution of $L\phi_\epsilon = 0$ of the form

$$\phi_\epsilon(v) = \mathbf{r}(v) \exp \left[-\frac{1}{\epsilon} \Phi(v) \right], \quad (3.12)$$

where \mathbf{r} is a $(N+1)$ -vector and $\Phi(v)$ is a scalar function. Substituting (3.12) into (3.7) yields an equation for Φ and \mathbf{r}

$$(A + \Phi' F) \mathbf{r} = \epsilon (F \mathbf{r})' + \lambda_0 \mathbf{r}. \quad (3.13)$$

Now substitute the asymptotic expansions $\mathbf{r} \sim \mathbf{r}_0 + \epsilon \mathbf{r}_1$ and $\Phi' \sim \Phi'_0 + \epsilon \Phi'_1$. Since, $\lambda_0 = \mathcal{O}(e^{-C/\epsilon})$, the leading order equation is

$$A \mathbf{r}_0 = -\Phi'_0 F \mathbf{r}_0, \quad (3.14)$$

For fixed v , this is equivalent to the generalized eigenvalue problem

$$A \psi = \mu F \psi, \quad (3.15)$$

where ψ is an eigenvector and μ is the corresponding eigenvalue. Indeed, we can define the eigenpair to be functions of v by requiring that they satisfy (3.15) for all $v \in (\vartheta_a, v_*)$. Then, after setting $\mathbf{r}_0 = \psi$ and $\Phi'_0 = \mu$, we have a solution to (3.13). Note that the generalized eigenvalue problem is equivalent to the standard eigenvalue problem

$$F^{-1} A \psi = \mu \psi, \quad (3.16)$$

so long as F is nonsingular, which is true for almost every $v \in (\vartheta_a, \vartheta_b)$.

The matrices A and M share the same nullspace, which is spanned by the nullvector $\boldsymbol{\rho}$ given by (2.24). We therefore set $\mu_0 = 0$ and $\psi_0 = \boldsymbol{\rho}$. Recall, that the nullvector $\boldsymbol{\rho}$ is positive and we define it to be the voltage-clamped steady-state distribution by normalizing it so that it sums to unity. For consistency, we assume that all of the right eigenvectors are similarly normalized. It can be shown [23] that there is one other positive eigenvector, which we define as ψ_1 . The corresponding eigenvalue, μ_1 , is nonzero for all values of $v \in (\vartheta_a, \vartheta_b)$ except for the deterministic fixed points v_0 and v_* . Furthermore, the sign of μ_1 is such that

$$\mu_1(v) > 0, \quad \text{for } \vartheta_a < v < v_0 \quad (3.17)$$

$$\mu_1(v) < 0, \quad \text{for } v_0 < v < v_*. \quad (3.18)$$

As we verify in Appendix A, the eigenvector ψ_1 is

$$(\psi_1)_n = f^{-N} \binom{N}{n} h^{N-n} g^n, \quad (3.19)$$

and the eigenvalue is

$$\mu_1 = \frac{N(af - g)}{bgh}, \quad (3.20)$$

where $h(v) = f(v) - g(v)$. We refer to the function Φ_0 as the stability landscape, which is

$$\begin{aligned} \Phi_0(v) &= - \int_{v_*}^v \mu_1(y) dy \\ &= \frac{N}{g'} \alpha(\vartheta_a) \left(E_i \left(\frac{2}{v_2} (v - \vartheta_a) \right) - E_i \left(\frac{2}{v_2} (v_* - \vartheta_a) \right) \right) \\ &\quad - \frac{N}{h'} (\log(\vartheta_b - v) - \log(\vartheta_b - v_*)), \end{aligned} \quad (3.21)$$

where $\alpha(v)$ is defined by (2.21) and $E_i(x)$ is the exponential integral function defined as the Cauchy principle value integral

$$E_i(x) = \int_{-\infty}^x t^{-1} e^t dt, \quad x \neq 0. \quad (3.22)$$

Collecting terms of $\mathcal{O}(\epsilon)$ in (3.13) yields

$$(A + \Phi'_0 F) \mathbf{r}_1 = (F \mathbf{r}_0)' - \Phi'_1 F \mathbf{r}_0. \quad (3.23)$$

Since $\mathbf{r}_0 = \psi_1$ and $\Phi'_0 = -\mu_1$ we get

$$\Phi'_1 = \frac{\boldsymbol{\eta}_1^T (F \psi_1)'}{\boldsymbol{\eta}_1^T F \psi_1}, \quad (3.24)$$

where $\boldsymbol{\eta}_1$ is the left nullvector of $(A - \mu_1 F)$ with components

$$(\boldsymbol{\eta}_1)_n = \left(\frac{a(f - g)}{bg} \right)^{N-n}. \quad (3.25)$$

After some calculation we find that

$$\Phi_1'(v) = (N-1)\mathcal{H}(v) - \frac{Nf'}{f(v)} + \frac{g'}{g(v)} + \frac{h'}{h(v)}, \quad (3.26)$$

$$\mathcal{H}(v) \equiv \frac{a(v)h(v)h' + b(v)g(v)g'}{a(v)h(v)^2 + b(v)g(v)^2}. \quad (3.27)$$

In jump Markov processes of this type, the function $\Phi_1(v)$ is small and can usually be ignored. However, a unique feature of the current model is that Φ_1 is N dependent and thus can contribute significantly to the solution. We note that $\Phi_1'(v)$ is independent of N at $v = v_0, v_*$, with

$$\lim_{v \rightarrow v_0, v_*} \Phi_1'(v) = \left[\frac{a(v)^2 h' + b(v)^2 g'}{a(v)b(v)f(v)} \right]_{v=v_0, v_*}. \quad (3.28)$$

Define

$$\omega(v) \equiv \exp \left[- \int_{v_*}^v \Phi_1(y) dy \right]. \quad (3.29)$$

Combining these results, the approximation of the eigenfunction, to leading order in ϵ , is

$$\phi_\epsilon(v) = \mathcal{N} \omega(v) \exp \left[- \frac{1}{\epsilon} \Phi_0(v) \right] \psi_1(v), \quad (3.30)$$

where \mathcal{N} is an unknown normalization factor.

If we think of this eigenfunction as a perturbation of the stationary distribution, when there is a reflecting boundary condition at v_* so that $\lambda_0 = 0$, then the scale factor, \mathcal{N} , can be set by normalizing $\phi_\epsilon(v)$ so that it integrates to unity. We can also think of this as enforcing conservation of probability with a modified initial condition. Notice that by integrating the initial condition (2.12) we have that

$$\sum_{n=0}^N \int_{\vartheta_a}^{v_*} p_n(v, 0) dv = 1. \quad (3.31)$$

Initially, the exact solution must have some probability contained within the other eigenfunctions, which means the approximation is not valid for small times. To ensure the approximate solution is valid for long time scales, we must modify the true initial condition (2.12) so that the approximation conserves probability correctly; that is, we must have that at $t = 0$, the probability that an action potential has not yet been initiated is unity. By setting $t = 0$ in (3.9), we see that this requirement also applies to the eigenfunction. This is equivalent to modifying the initial conditions so that the process starts on the stationary distribution, which generates a small error because convergence to the stationary distribution is fast compared to initiation of an action potential. The normalization constant is then

$$\mathcal{N} = \left[\int_{\vartheta_a}^{v_*} \omega(v) \exp \left[- \frac{1}{\epsilon} \Phi_0(v) \right] dv \right]^{-1}, \quad (3.32)$$

which can be approximated using Laplace's method [25], to get

$$\mathcal{N} \sim \frac{1}{\omega(v_0)} \sqrt{\frac{|\mu_1'(v_0)|}{2\pi\epsilon}} \exp \left[- \frac{1}{\epsilon} \Phi_0(v_0) \right]. \quad (3.33)$$

B. Eigenvalue approximation

To estimate the eigenvalue, λ_0 , we project using the adjoint eigenfunction ξ_0 , which satisfies

$$L^* \xi_0 \equiv -F \frac{d\xi_0}{dv} - A^T \xi_0 = \lambda_0 \xi_0, \quad (3.34)$$

$$(\xi_0)_n(v_*) = 0, \quad \text{for } n = k, \dots, N. \quad (3.35)$$

Consider the identity

$$\langle \phi_0, L^* \xi_0 \rangle = \lambda_0 \langle \phi_0, \xi_0 \rangle, \quad (3.36)$$

where the inner product is defined by

$$\langle \mathbf{u}, \mathbf{w} \rangle \equiv \int_{\vartheta_a}^{v_*} \mathbf{u}(v)^T \mathbf{w}(v) dv. \quad (3.37)$$

To leading order in ϵ we have that $\phi_0 \sim \phi_\epsilon$ and $L\phi_\epsilon = 0$. Substituting this approximation into (3.36) and applying integration by parts yields

$$\begin{aligned} \lambda_0 &\sim - \frac{\xi_0(v_*)^T F(v_*) \phi_\epsilon(v_*)}{\langle \xi_0, \phi_\epsilon \rangle} \\ &\sim - \mathcal{N} \xi_0(v_*)^T F(v_*) \psi_1(v_*). \end{aligned} \quad (3.38)$$

In the absence of an absorbing boundary condition the left eigenfunction is $\xi_0 = \mathbf{1}$; however, substitution into (3.38) yields $\lambda_0 = 0$ since neither approximation accounts for the boundary condition. Thus, we must construct an approximation for ξ_0 which satisfies (3.35).

Since λ_0 is exponentially small, we seek an approximation to ξ_0, ξ_ϵ say, which satisfies

$$\epsilon F \frac{d\xi_\epsilon}{dv} + A^T \xi_\epsilon = 0, \quad (3.39)$$

the boundary condition (3.35), and

$$\lim_{\epsilon \rightarrow 0} \xi_\epsilon(v) = \mathbf{1} \quad (3.40)$$

for $v \in (\vartheta_a, v_*)$.

In general, the solution of (3.39) can be approximated by a superposition of eigenvectors, η_j , of the matrix $F^{-1}A^T$, which have corresponding eigenvalues μ_j , $j = 0, \dots, N$. We remind the reader that all of these quantities depend on the voltage v . Consider a solution to (3.35) of the form

$$\xi_\epsilon(v) = c_j(v) \eta_j(v). \quad (3.41)$$

Substitution into (3.35) yields

$$(\epsilon c_j' + \mu_j c_j) F \eta_j + \epsilon c_j F \eta_j' = 0. \quad (3.42)$$

This can be thought of as a way of generalizing the WKB method used above to approximate the eigenfunction ϕ_0 .

The approximate solution (3.41) will be accurate, to leading order in ϵ , if we require the function $c_j(v)$ to satisfy the linear equation

$$\epsilon c'_j + \mu_j(v) c_j = 0. \quad (3.43)$$

Recall there is always one zero eigenvalue given by $\mu_0 = 0$, with eigenvector $\boldsymbol{\eta}_0 = \mathbf{1}$, so that

$$\epsilon c_0(v)' = 0, \quad (3.44)$$

implying a constant solution. A full solution can then be written as

$$\boldsymbol{\xi}_\epsilon(v) = c_0 \mathbf{1} + c_1(v) \boldsymbol{\eta}_1(v) + \sum_{n=2}^N c_n(v) \boldsymbol{\eta}_n(v). \quad (3.45)$$

However, not all eigenvectors will result in bounded solutions. We expect that away from the absorbing boundary the solution should be very close to $\mathbf{1}$, which means that we are interested in the solutions in the vicinity of $v \leq v_*$. For $j \geq 2$, the only bounded solutions are those for which $\mu_j(v_*)$ has negative real part. It can be shown [23] that the sign of the real part of the eigenvalues is determined by the number of negative components of $\mathbf{f}(v_*)$ (recall that we have defined k (3.2) to be this number). In particular, at the absorbing boundary, $v = v_*$, there are $N - k$ eigenvalues of $F(v_*)^{-1} A(v_*)^T$ with negative real part. These we denote by μ_j , $j = 2, \dots, N - k + 1$. The remaining $k - 1$ eigenvalues have positive real part. Thus, we take $c_j = 0$ for $j = N - k + 2, \dots, N$, and

$$c_j(v) = C_j \exp \left[\frac{\mu_j(v_*)(v - v_*)}{\epsilon} \right], \quad (3.46)$$

for $j = 2, \dots, N - k + 1$.

To leading order in ϵ , the equation for $c_1(v)$ is similar, namely

$$\epsilon c'_1 + \mu_1 c_1 = 0, \quad (3.47)$$

however, since $\mu_1(v_*) = 0$ (see Eqn. (3.20)) its behavior in the vicinity of v_* is not exponential, but rather

$$c_1(v) = C_1 \exp \left[\frac{-\mu'_1(v_*)(v - v_*)^2}{2\epsilon} \right]. \quad (3.48)$$

Note that since $\mu'_1(v_*) > 0$, this is exponentially small away from the boundary.

At first (3.45) would seem to be a plausible approximation to the eigenfunction, but a hidden assumption in this solution is that the matrix $F^{-1} A^T$ is diagonalizable. However, because $\mu_1 \rightarrow 0$ and $\boldsymbol{\eta}_1 \rightarrow \mathbf{1}$ as $v \rightarrow v_*$ (see Eqn. (3.25)) the eigenspace corresponding to the zero eigenvalue is degenerate at $v = v_*$ (having algebraic multiplicity two and geometric multiplicity one) and the solution needs to include the generalized nullvector,

$$\boldsymbol{\zeta}^T \equiv \mathbf{f}(v_*)^T A(v_*)^\dagger. \quad (3.49)$$

To that end we try a partial solution of (3.39) of the form

$$\boldsymbol{\xi}_\epsilon(v) = c_0(v) \mathbf{1} + c_1(v) \boldsymbol{\omega}(v), \quad (3.50)$$

where

$$\boldsymbol{\omega}(v) = \frac{1}{\nu(v)} (\boldsymbol{\eta}_1(v) - \mathbf{1}). \quad (3.51)$$

Notice that

$$A^T \boldsymbol{\omega} = \frac{\mu_1}{\nu} F \boldsymbol{\eta}_1, \quad (3.52)$$

so that

$$\lim_{v \rightarrow v_*} \boldsymbol{\omega} = \frac{\mu'_1(v_*)}{\nu'(v_*)} \boldsymbol{\zeta}. \quad (3.53)$$

Substituting (3.50) into (3.39), we find

$$\epsilon F \frac{d}{dv} (c_0 \mathbf{1} + c_1 \boldsymbol{\omega}) + A^T (c_1 \boldsymbol{\omega}) = 0, \quad (3.54)$$

and after using (3.51) we get

$$\frac{1}{\nu} (\epsilon c'_1 + \mu_1 c_1) F \boldsymbol{\eta}_1 + \epsilon \left(c'_0 - \frac{c'_1}{\nu} \right) \mathbf{f} = -\epsilon c_1 F \boldsymbol{\omega}'. \quad (3.55)$$

Comparing this with (3.42) it is clear that more care must be taken as we now have terms divided by $\nu(v)$, which vanishes at v_0 and v_* . Therefore, we must make sure that the error terms vanish sufficiently fast in the limit $v \rightarrow v_{0,*}$.

We consider now the full solution

$$\boldsymbol{\xi}_\epsilon(v) = c_0(v) \mathbf{1} + c_1(v) \boldsymbol{\omega}(v) + \sum_{j=2}^{N-k+1} c_j(v) \boldsymbol{\eta}_j(v). \quad (3.56)$$

Our strategy will be to project the above solution with the set of eigenvectors $\{\boldsymbol{\psi}_j\}$, $j = 0, 1, \dots, N$, of the matrix $F^{-1} A$, which forms an biorthogonal set with the eigenvectors $\boldsymbol{\eta}_j$ in the sense that $\boldsymbol{\psi}_i^T F \boldsymbol{\eta}_j = \delta_{i,j}$. If the error remains bounded for each of the $N + 1$ resulting equations then we can be sure it is bounded in general. We note that this is not unlike the procedure for computing Fourier coefficients in a series expansion. Substituting (3.56) into (3.39), we find

$$\begin{aligned} \epsilon F \frac{d}{dv} \left(c_0 \mathbf{1} + c_1 \boldsymbol{\omega} + \sum_{j=2}^{N-k+1} c_j \boldsymbol{\eta}_j \right) \\ = -A^T \left(c_1 \boldsymbol{\omega} + \sum_{j=2}^{N-k+1} c_j \boldsymbol{\eta}_j \right). \end{aligned} \quad (3.57)$$

Taking the product of this expression with $\boldsymbol{\psi}_0^T = \boldsymbol{\rho}^T$ we find

$$c'_0 \nu = c'_1 - c_1 \boldsymbol{\rho}^T F \boldsymbol{\omega}' - \sum_{j=2}^{N-k+1} c_j \boldsymbol{\rho}^T F \boldsymbol{\eta}'_j, \quad (3.58)$$

where we have used that $\boldsymbol{\rho}^T F \boldsymbol{\omega} = -1$. Similarly, taking the product with $\boldsymbol{\psi}_i^T$ gives

$$\begin{aligned} \epsilon \boldsymbol{\psi}_i^T F \left(c'_0 \mathbf{1} + c'_1 \boldsymbol{\omega} + \sum_{j=2}^{N-k+1} c'_j \boldsymbol{\eta}_j + c_1 \boldsymbol{\omega}' + \sum_{j=2}^{N-k+1} c_j \boldsymbol{\eta}'_j \right) \\ = -\mu_i \boldsymbol{\psi}_i^T F \left(c_1 \boldsymbol{\omega} + \sum_{j=2}^{N-k+1} c_j \boldsymbol{\eta}_j \right). \end{aligned} \quad (3.59)$$

For $i \geq 2$ this reduces to

$$c'_i + \frac{\mu_i}{\epsilon} c_i + c_1 \frac{\boldsymbol{\psi}_i^T F \boldsymbol{\omega}'}{\boldsymbol{\psi}_i^T F \boldsymbol{\eta}_i} + \sum_{j=2}^{N-k+1} c_j \frac{\boldsymbol{\psi}_i^T F \boldsymbol{\eta}'_j}{\boldsymbol{\psi}_i^T F \boldsymbol{\eta}_i} = 0, \quad (3.60)$$

while for $i = 1$ we find

$$c'_1 + c_1 \left(\frac{\mu_1}{\epsilon} + \frac{\boldsymbol{\psi}_1^T F \boldsymbol{\omega}'}{\boldsymbol{\psi}_1^T F \boldsymbol{\omega}} \right) + \sum_{j=2}^{N-k+1} c_j \frac{\boldsymbol{\psi}_1^T F \boldsymbol{\eta}'_j}{\boldsymbol{\psi}_1^T F \boldsymbol{\omega}} = 0. \quad (3.61)$$

Since $\boldsymbol{\psi}_1^T F \boldsymbol{\omega} \rightarrow \boldsymbol{\rho}^T F \boldsymbol{\omega} = -1$ as $v \rightarrow v_*$, the higher order terms in the above expression remain bounded. Substituting (3.61) into (3.58) we find

$$\begin{aligned} c'_0 \nu = -c_1 \left(\frac{1}{\epsilon} \mu_1 + \frac{\boldsymbol{\psi}_1^T F \boldsymbol{\omega}'}{\boldsymbol{\psi}_1^T F \boldsymbol{\omega}} + \boldsymbol{\rho}^T F \boldsymbol{\omega}' \right) \\ - \sum_{j=2}^{N-k+1} c_j \left(\frac{\boldsymbol{\psi}_1^T F \boldsymbol{\eta}'_j}{\boldsymbol{\psi}_1^T F \boldsymbol{\omega}} + \boldsymbol{\rho}^T F \boldsymbol{\eta}'_j \right). \end{aligned} \quad (3.62)$$

Now, since $\boldsymbol{\psi}_1 \rightarrow \boldsymbol{\rho}$ as $v \rightarrow v_*$ (see Eqn. (2.24) and (3.19)) we define the vector $\boldsymbol{\chi}$ such that $\boldsymbol{\psi}_1 = \boldsymbol{\rho} - \nu \boldsymbol{\chi}$ and write

$$\begin{aligned} c'_0 = -c_1 \left(\frac{1}{\epsilon} \frac{\mu_1}{\nu} + \frac{\boldsymbol{\chi}^T F \boldsymbol{\omega}' + (\boldsymbol{\chi}^T F \boldsymbol{\omega})(\boldsymbol{\rho}^T F \boldsymbol{\omega}')}{1 + \nu \boldsymbol{\chi}^T F \boldsymbol{\omega}} \right) \\ - \sum_{j=2}^{N-k+1} c_j \left(\frac{\boldsymbol{\chi}^T F \boldsymbol{\eta}'_j + (\boldsymbol{\chi}^T F \boldsymbol{\omega})(\boldsymbol{\rho}^T F \boldsymbol{\eta}'_j)}{1 + \nu \boldsymbol{\chi}^T F \boldsymbol{\omega}} \right). \end{aligned} \quad (3.63)$$

It is evident that the higher order terms in the above equation are bounded as $v \rightarrow v_*$. From (3.61) we see that $c_1(v)$ is still given by (3.48), but instead of c_0 being constant, from (3.63) we have

$$c_0(v) = C_0 + C_1 \frac{1}{\epsilon} \frac{\mu'_1(v_*)}{\nu'(v_*)} \int_v^{v_*} \exp \left[\frac{-\mu'_1(v_*)(s - v_*)^2}{2\epsilon} \right] ds. \quad (3.64)$$

Now that we have a uniform solution, we must resolve the undetermined constants C_j using the boundary condition and (3.40). For any fixed $v < v_*$ and $\epsilon \rightarrow 0$,

$$c_0(v) \sim C_0 + C_1 \frac{1}{\nu'(v_*)} \sqrt{\frac{\pi \mu'_1(v_*)}{2\epsilon}}, \quad (3.65)$$

so we require

$$C_0 + C_1 \frac{1}{\nu'(v_*)} \sqrt{\frac{\pi \mu'_1(v_*)}{2\epsilon}} = 1. \quad (3.66)$$

Finally, we need to satisfy the boundary conditions at $v = v_*$. Although the number k is specified (see Eqn. (3.2)) a good approximation for the eigenvalue can still be obtained if we assume that $k = N$; this gives

$$C_1 \frac{\mu'_1(v_*)}{\nu'(v_*)} \zeta_N + C_0 = 0, \quad (3.67)$$

which implies that

$$C_1 = \nu'(v_*) \sqrt{\frac{2\epsilon}{\pi \mu'_1(v_*)}}, \quad C_0 = -\zeta_N \sqrt{\frac{2\epsilon \mu'_1(v_*)}{\pi}}, \quad (3.68)$$

to leading order in ϵ .

To compute the eigenvalue λ_0 , we need

$$\boldsymbol{\xi}_\epsilon(v_*) = C_1 \frac{\mu'_1(v_*)}{\nu'(v_*)} \boldsymbol{\zeta} - \zeta_N \mathbf{1}. \quad (3.69)$$

Because $\mathbf{1}^T F \boldsymbol{\psi}_1 = 0$, substitution of (3.69) into (3.38) yields

$$\lambda_0 \sim C_1 \frac{\mu'_1(v_*)}{\nu'(v_*)} \omega(v_0) B(v_*) \mathcal{N}, \quad (3.70)$$

where

$$B(v) \equiv -\mathbf{f}^T A^\dagger F \boldsymbol{\rho} = \frac{1}{N} a(v) b(v)^2 f(v)^2. \quad (3.71)$$

Thus, the eigenvalue is

$$\lambda_0 \sim \frac{B(v_*)}{\pi \omega(v_0)} \sqrt{|\Phi_0''(v_0)| \Phi_0''(v_*)} \exp \left[-\frac{1}{\epsilon} \Phi_0(v_0) \right]. \quad (3.72)$$

IV. THE QSS REDUCTION

To approximate the MFT for stimulus current above threshold ($I > I_*$), we can approximate the discrete channel noise with an effective continuous Markov process. That is, we replace the CK equation (2.23) with an effective FP equation. To derive the FP equation, we exploit the fact that the ion channels that drive the action potential are “fast” channels, in that their open and close rates are typically large compared to other processes.

We begin by splitting \mathbf{p} into two parts

$$\mathbf{p} = u \boldsymbol{\rho} + \mathbf{w}, \quad (4.1)$$

where $\mathbf{1}^T \mathbf{p} = u$, and $\mathbf{1}^T \mathbf{w} = 0$. It follows that

$$\frac{\partial u}{\partial t} = -\mathbf{1}^T \frac{\partial}{\partial v} (F(u \boldsymbol{\rho} + \mathbf{w})), \quad (4.2)$$

and

$$\frac{\partial \mathbf{w}}{\partial t} = \frac{1}{\epsilon} A \mathbf{w} - \frac{\partial}{\partial v} (F \boldsymbol{\rho}) + \mathbf{1}^T \frac{\partial}{\partial v} (F \boldsymbol{\rho}) \boldsymbol{\rho}. \quad (4.3)$$

Here, the fast behavior of \mathbf{w} is evident, so we take \mathbf{w} to be in quasi-steady state. Thus, we take

$$A \mathbf{w} = \epsilon \frac{\partial}{\partial v} (u F \boldsymbol{\rho}) - \epsilon \mathbf{1}^T \frac{\partial}{\partial v} (u F \boldsymbol{\rho}) \boldsymbol{\rho} + O(\epsilon^2). \quad (4.4)$$

The Fredholm alternative theorem [25] guarantees that this equation can be solved uniquely for \mathbf{w} subject to the constraint $\mathbf{1}^T \mathbf{w} = 0$; we denote this solution as

$$\mathbf{w} = \epsilon A^\dagger \frac{\partial}{\partial v} (u F \boldsymbol{\rho}) - \epsilon A^\dagger \mathbf{1}^T \frac{\partial}{\partial v} (u F \boldsymbol{\rho}) \boldsymbol{\rho} + O(\epsilon^2), \quad (4.5)$$

where A^\dagger is the inverse of the properly constrained A . Consequently, ignoring terms of order ϵ^2 ,

$$\begin{aligned} \frac{\partial u}{\partial t} = & -\frac{\partial}{\partial v} \left(\epsilon \mathbf{1}^T F A^\dagger \frac{\partial}{\partial v} ((F \boldsymbol{\rho} - \mathbf{1}^T (F \boldsymbol{\rho}) \boldsymbol{\rho}) u) \right) \\ & - \frac{\partial}{\partial v} (\mathbf{1}^T F \boldsymbol{\rho} u), \end{aligned} \quad (4.6)$$

a Fokker-Planck equation. Rewriting this equation, we have

$$\frac{\partial u}{\partial t} = -\frac{\partial}{\partial v} (\nu u) + \epsilon \frac{\partial}{\partial v} \left(B \frac{\partial u}{\partial v} \right), \quad (4.7)$$

where ν and B are defined by (2.25) and (3.71), respectively. The corresponding Stratonovich SDE is

$$dV = \nu(V)dt + \sqrt{2\epsilon B(V)} * dW. \quad (4.8)$$

A. Mean first passage time problem

It is well known that the mean first passage time (MFPT) $T(v)$ for a time-autonomous process satisfies the ordinary differential equation

$$\nu(v) \frac{dT}{dv} + \frac{d}{dv} \left(B(v) \frac{dT}{dv} \right) = -1, \quad (4.9)$$

For our problem, we impose the boundary conditions

$$T'(\vartheta_a) = 0, \quad T(\vartheta_1) = 0. \quad (4.10)$$

The left reflecting boundary is required because the voltage can never drop below ϑ_a (2.17), and we take the exit point to be ϑ_1 (2.18) because this defines the threshold in the deterministic problem.

It can be shown that the solution to (4.9) is given by

$$T(v) = \int_v^{\vartheta_1} dy \exp[-\Psi(y)] \int_{\vartheta_a}^y \frac{dz}{B(z)} \exp[\Psi(z)], \quad (4.11)$$

where

$$\Psi(v) = \int_{\vartheta_a}^v \frac{\nu(v') + B'(v')}{B(v')} dv'. \quad (4.12)$$

However, in most cases, the integrals cannot be explicitly evaluated, and numerical methods must be employed.

Rather than using numerical integration methods to evaluate (4.11), it is straightforward to solve the boundary value problem numerically using a shooting method. We let $T(v) = \hat{T}(v) + c$, where c is a constant. Then, $\hat{T}(v)$ is the solution of the equation (4.9), and the boundary

conditions (4.10) can be imposed as the initial conditions $\hat{T}(\vartheta_a) = 0$ and $\hat{T}'(\vartheta_a) = 0$. After setting $c = -\hat{T}(\vartheta_1)$, we recover the desired solution. This converts the BVP to an IVP, which can be efficiently and accurately solved using standard stiff ODE solvers. The mean of the RV, T , gives us a great deal of information, but it is worth mentioning that for $I > I_*$ and large N , the density function for T is asymptotically Gaussian, where the mean is given by the deterministic limit [11].

In the case where $I < I_*$ the MFPT becomes the mean exit time for a spontaneous action potential, for which the QSS approximation is defined but is inaccurate. In this case (4.11) can be approximated along the lines of standard Kramers theory. There are many methods for obtaining this approximation too numerous to restate here. We simply quote the result and direct the interested reader to [4, 14]. We have that $\mathcal{F}(t) \sim e^{-\lambda_{qss} t}$, where $T \sim 1/\lambda_{qss}$ and

$$\lambda_{qss} \sim \frac{B(v_*)}{\pi} \sqrt{\left| \frac{\nu'(v_0)}{B(v_0)} \right| \left| \frac{\nu'(v_*)}{B(v_*)} \right|} \exp \left[\frac{1}{\epsilon} \int_{v_0}^{v_*} \frac{\nu(y)}{B(y)} dy \right]. \quad (4.13)$$

Comparing this to the quasi-stationary approximation (3.72) we can see that the prefactors differ by the quantity $1/\omega(v_0)$, which is an exponential function of N (see (3.29) and (3.26)). However, the largest contribution to the error in the MFT is the error in the estimate of the stability well (compare $\int_{v_*}^v \mu_1(v') dv' = \int_{v_*}^v \frac{\nu(v')}{b(v')g(v')h(v')} dv'$ to $\int_{v_*}^v \frac{\nu(v')}{B(v')} dv'$) because this generates errors that are exponential in N/ϵ .

V. THE SYSTEM-SIZE EXPANSION

In this section we ask the following question. Can we replace the SDE (2.8), which is driven by discrete channel noise, by two coupled SDEs, like (1.6), for the variables V and S , where the channel noise is continuous? This is different than the QSS reduction, which resulted in the single SDE (4.8) for the variable V . Instead of exploiting fast channel switching, the system-size expansion [26] relies on the presence of a large number of channels $N \gg 1$. An alternative method for deriving this approximation begins with the Kramers-Moyal expansion, which is an expansion in the moments of the discrete jump propagator. One can only truncate this expansion at the second moment by linearizing around the deterministic stable critical point, that is, the stable critical point in the variable s , which we distinguish from the fixed points in the variable v . It can be shown that the result is the same as that obtained by the direct system-size expansion [5]. The benefit of using the system-size expansion is that more complicated conductance models—such as the Hodgkin-Huxley model—can be treated analytically. However, as we show in this section, the system-size expansion only gives a good approximation for the mean firing time when $I > I_*$. Moreover,

at least for the Morris-Lecar model considered here, the QSS (or adiabatic) reduction of the FP equation obtained by the system-size expansion is identical to the QSS reduction of the full model.

The Krammers-Moyal expansion of (2.11) is found by setting $s = \frac{n}{N}$, with $ds = \frac{1}{N}$. We then expand in small ds about $s = a(v)$ (the deterministic critical point) to find

$$\frac{\partial p}{\partial t} = -\frac{\partial}{\partial v}((sf - g)p) + \frac{1}{\epsilon} \left(\frac{\partial}{\partial s} \left(\frac{s-a}{b} p \right) + \frac{a}{N} \frac{\partial^2 p}{\partial s^2} \right), \quad (5.1)$$

It is evident that the discrete matrix operator A is replaced by a differential operator in the variable s . In this section, we first compute the QSS reduction of the above equation, which is also known in the literature as the adiabatic reduction [5]. Then, we apply the WKB method to approximate the stationary distribution. In each case, we compare the results with those obtained for the discrete equations.

A. Adiabatic reduction

First, we make the following change of variables. We set $x = s - a$, $v = y$, and

$$D(y) = \frac{a(y)}{N}, \quad c(y) = \frac{1}{b(y)}, \quad \nu(y) = a(y)f(y) - g(y), \quad (5.2)$$

to get the system

$$\frac{\partial p}{\partial t} = -\frac{\partial}{\partial y}((f(y)x + \nu(y))p) + \frac{1}{\epsilon} \frac{\partial}{\partial x}(c(y)xp + D(y)\frac{\partial p}{\partial x}). \quad (5.3)$$

The method can be presented best using operator notation. We define the linear operators

$$L_1 p = \frac{\partial}{\partial x} \left(c x p + D \frac{\partial p}{\partial x} \right), \quad L_2 p = -\frac{\partial}{\partial y} (f x p), \quad (5.4)$$

$$L_3 = -\frac{\partial}{\partial y} (\nu p). \quad (5.5)$$

We want a projection operator based on the null-space of L_1 . Note that $L_1 \rho = 0$ implies that

$$D \rho' + c x \rho = 0, \quad (5.6)$$

so that

$$\rho(x | y) = \sqrt{\frac{c}{2\pi D}} \exp\left(-\frac{cx^2}{2D}\right), \quad (5.7)$$

and $\int_{-\infty}^{\infty} \rho dx = 1$. Notice that ρ depends on y because c and D are functions of y . The adjoint operator has a null space spanned by $\eta = 1$, so the projection operator we seek is

$$\mathcal{P}q = \rho(x | y) \int_{-\infty}^{\infty} q(x, y) dx. \quad (5.8)$$

Now, we set $p = \mathcal{P}p + (1 - \mathcal{P})p = r + \epsilon w$ (so that $\mathcal{P}p = r = u(y, t)\rho(x | y)$) and observe that

$$\begin{aligned} L_2 r &= -\frac{\partial}{\partial y} (f x \mathcal{P}p) = -\frac{\partial}{\partial y} (f x u \rho) \\ L_3 r &= -\frac{\partial}{\partial y} (\nu u \rho) \end{aligned} \quad (5.9)$$

Since $\int_{-\infty}^{\infty} x \rho dx = 0$, we also observe that

$$\mathcal{P}L_2 r = 0, \quad \mathcal{P}L_3 r = -\rho \frac{\partial}{\partial y} (\nu u). \quad (5.10)$$

Furthermore, we assume that p decays sufficiently fast as $x \rightarrow \pm\infty$ so that $\mathcal{P}L_1 p = 0$.

Applying the projection operator to both sides of (5.3) yields

$$\frac{\partial r}{\partial t} = \mathcal{P} \left(\frac{1}{\epsilon} L_1 + L_2 + L_3 \right) (r + \epsilon w) = \mathcal{P}L_3 r + \epsilon \mathcal{P}L_2 w. \quad (5.11)$$

On the other hand, if we apply the projection $1 - \mathcal{P}$ to (5.3), we get

$$\epsilon \frac{\partial w}{\partial t} = L_1 w + (1 - \mathcal{P})(L_2 + L_3)r + \epsilon(1 - \mathcal{P})(L_2 + L_3)w. \quad (5.12)$$

Now, we assume that w is at a quasi-steady-state, so take

$$L_1 w = -(1 - \mathcal{P})(L_2 + L_3)r. \quad (5.13)$$

It can be shown that contributions to w that determine the $\mathcal{O}(\epsilon)$ diffusivity in the final FP equation depend only on L_2 . Although contributions from L_3 affect the drift term, they are higher order and can be ignored. The solution can then be formally written as

$$w = -L_1^{-1}(1 - \mathcal{P})L_2 r, \quad (5.14)$$

which is substituted into (5.11) to get the FP equation

$$\frac{\partial r}{\partial t} = \mathcal{P}L_3 r - \epsilon \mathcal{P}L_2 L_1^{-1}(1 - \mathcal{P})L_2 r. \quad (5.15)$$

We need only solve for w , given by (5.14). To do this we use the following properties of ρ :

$$x \rho = -\frac{D}{c} \frac{\partial \rho}{\partial x}, \quad \frac{\partial \rho}{\partial y} = -\frac{1}{2} \frac{d}{dy} \log(D/c) \left(1 - \frac{c}{D} x^2\right) \rho. \quad (5.16)$$

The goal is to express $(1 - \mathcal{P})L_2 r$ in terms of total derivatives with respect to x . First, we substitute (5.9) into the RHS of (5.13). Then, we use (5.16) to get

$$\frac{\partial}{\partial x} (c x w + D \frac{\partial w}{\partial x}) = -\frac{\partial}{\partial y} \left(\frac{f D}{c} \frac{\partial \rho}{\partial x} u \right). \quad (5.17)$$

After integrating and rearranging the above equation we have

$$D \frac{\partial}{\partial x} \left(\frac{w}{\rho} \right) = -\frac{1}{\rho} \frac{\partial}{\partial y} \left(\frac{f D}{c} u \rho \right). \quad (5.18)$$

Differentiating the RHS of (5.18) and using (5.16) then yields

$$D \frac{\partial}{\partial x} \left(\frac{w}{\rho} \right) = - \frac{\partial}{\partial y} \left(\frac{fD}{c} u \right) + \frac{1}{2} \frac{d}{dy} \left(\frac{D}{c} \right) \left(1 - \frac{c}{D} x^2 \right) \frac{fD}{c} u. \quad (5.19)$$

We can integrate both sides of the result to get

$$w = - \left[\frac{1}{D} \frac{\partial}{\partial y} \left(\frac{fD}{c} u \right) + \frac{1}{2} \frac{d}{dy} \left(\frac{D}{c} \right) \left(1 - \frac{cx^2}{3D} \right) \frac{f}{c} u \right] x \rho, \quad (5.20)$$

which is then substituted into the final term of (5.15)

$$\mathcal{P}L_2 w = \rho \frac{\partial}{\partial y} \left(\frac{f}{c} \frac{\partial}{\partial y} \left(\frac{fD}{c} u \right) \right). \quad (5.21)$$

Then, by dividing (5.15) through by ρ , we get an equation for the scalar function u :

$$\frac{\partial u}{\partial t} = - \frac{\partial}{\partial y} (\nu u) + \epsilon \frac{\partial}{\partial y} \left(\frac{f^2 D}{c^2} \frac{\partial u}{\partial y} \right), \quad (5.22)$$

where we have ignored the $\mathcal{O}(\epsilon)$ terms in the drift velocity.

Expressing this in terms of the original variables, we find that, to leading order, the resulting FP equation is exactly the same as equation (4.7) derived previously from the discrete model.

B. WKB approximation of the stationary distribution

The above analysis shows that the adiabatic reduction applied after the system-size expansion is identical to the QSS reduction applied to the full discrete model. However, as we show in this section, the WKB approximation of the stationary distribution of (5.1) is not consistent with the approximation of Section III; furthermore, the result is subject to the same large-deviation errors as the QSS reduction. As a result, the system-size expansion can only provide an accurate approximation for above-threshold stimulus current $I > I_*$.

It is no surprise that the leading-order WKB approximation is simply the continuum analogue of the discrete eigenvalue problem (3.14). The existence and uniqueness of the eigenpair (μ_1, ψ_1) is guaranteed in the discrete case, and we are interested as to whether these properties extend to the case of continuous noise. Our results provide strong evidence that this is indeed true.

We seek to approximate the solution to the equation

$$\frac{1}{\epsilon} \left[D(v) \frac{\partial^2 \hat{p}}{\partial s^2} + \frac{\partial}{\partial s} ((s - a(v)) \hat{p}) \right] = b(v) \frac{\partial}{\partial v} (sf(v) - g(v)) \hat{p}, \quad (5.23)$$

satisfying the normalization condition

$$\int_{-\infty}^{\infty} \int_0^1 \hat{p}(v, s) ds dv = 1, \quad (5.24)$$

where $D(v) = a(v)b(v)/N$. The solution is assumed to have the following form

$$\hat{p}(v, s) = r_0(v, s) \exp \left[-\frac{1}{\epsilon} \Phi_0(v) \right]. \quad (5.25)$$

After substituting this into (5.23) we have

$$[L + b\Phi'_0 F] r_0 = \epsilon b \frac{\partial}{\partial v} (F r_0), \quad (5.26)$$

where the operator L is defined as

$$L \equiv D(v) \frac{\partial^2}{\partial s^2} + (s - a(v)) \frac{\partial}{\partial s} + 1, \quad (5.27)$$

and $F(s, v) = sf(v) - g(v)$. Collecting terms of leading order in ϵ , we obtain the eigenvalue problem

$$[L + b\Phi'_0 F] r_0 = 0, \quad (5.28)$$

which is the continuum version of (3.14). Thus, up to an s -independent normalization factor, we have that $r_0(v, s) = \psi(s|v)$ and $\Phi'_0(v) = \mu(v)/b(v)$, where ψ and μ are the eigenpair for the generalized eigenvalue problem.

We wish to solve for the eigenfunction $\psi(s|v)$ and eigenvalue μ , which satisfy the equation

$$D\psi'' + (s - a)\psi' + (1 + \mu F)\psi = 0. \quad (5.29)$$

From (3.20) we know that the eigenvalue must vanish at a fixed point, where $a(v)f(v) - g(v) = 0$. If we set $\mu = 0$ in the above equation, we get an equation for the eigenfunction $\rho(s|v)$, with solution

$$\rho(s|v) = \exp \left[-\frac{(s - a(v))^2}{2D(v)} \right]. \quad (5.30)$$

This solution provides the essential property of zero flux, that is

$$D \frac{\partial \rho}{\partial s} + (s - a)\rho = 0. \quad (5.31)$$

Likewise, the eigenfunction ψ must satisfy this property, so we seek a solution of the form

$$\psi(s|v) = \exp \left[-\frac{(s - \kappa(v))^2}{2D(v)} \right], \quad (5.32)$$

where $\kappa(v)$ is an unknown shifted mean. After substituting into (5.29), we have

$$(s - \kappa)^2 - (s - a)(s - \kappa) + \mu D(sf - g) = 0. \quad (5.33)$$

Two equations for the two unknowns μ and κ are then obtained by expanding the above to get

$$(-\kappa + a + \mu Df)s + (\kappa^2 - a\kappa - \mu Dg) = 0, \quad (5.34)$$

and requiring each term to vanish so that

$$\kappa = a + \mu Df, \quad (5.35)$$

$$\kappa^2 = a\kappa + \mu Dg. \quad (5.36)$$

Solving these two equations yields either $\mu(v) = 0$ and $\kappa(v) = a(v)$, which recovers the function $\rho(s|v)$, or

$$\mu(v) = -N \frac{a(v)f(v) - g(v)}{a(v)b(v)f(v)^2}, \quad \kappa(v) = \frac{g(v)}{f(v)}. \quad (5.37)$$

The solution for the eigenfunction is then

$$\psi(s|v) = \exp \left[-\frac{(s - g(v)/f(v))^2}{2D(v)} \right], \quad (5.38)$$

which is a shifted version of the steady-state solution so that $\psi(s|v) = \rho(s - \zeta(v)|v)$, where the shift is $\zeta(v) = (g(v)/f(v) - a(v))$. Treating ψ as an approximation of the true eigenvector, given by (3.19), we can see that it cannot be uniformly accurate in v . The reason for this inaccuracy is simple; the system-size expansion results in approximations of the first and second moment of the jump propagator by linearizing them around the deterministic critical point $s = a$. While this creates no approximation for the first moment, since it is already linear in s , the second moment is frozen to its value at the critical point. Remember that this is the best that can be expected, since truncation of the Kramers-Moyal expansion at the second moment is valid only near the deterministic critical point. Away from the critical point, all moments of the propagator are significant. The function $\rho(s|v)$ is uniformly accurate because it is peaked at the critical point, where the system-size expansion is at its most accurate. However, since the peak of the eigenfunction $\psi(s|v)$ is shifted, it is only accurate for values of v such that $|\zeta(v)| \ll 1$; that is, near the fixed point v_0 , where $g(v_0) = a(v_0)f(v_0)$.

As for the eigenvalue approximation, we have that $\mu(v)/b(v) = -\nu(v)/B(v)$, where $\nu(v)$ is the mean total current and $B(v)$ is the diffusivity, defined by (2.25) and (3.71). The true eigenvalue, given by (3.20), differs from the approximation only in the denominator; that is, ignoring the common factor of b , the estimate from (5.37) has the denominator abf^2 , whereas the true denominator is $g(f - g)$. Now, notice that at the fixed point $v = v_0$, where $g(v_0) = a(v_0)f(v_0)$, we have

$$\begin{aligned} g(v_0)(f(v_0) - g(v_0)) &= a(v_0)f(v_0)(1 - a(v_0))f(v_0) \\ &= a(v_0)b(v_0)f(v_0)^2. \end{aligned} \quad (5.39)$$

Thus, like the eigenfunction $\psi(s|v)$, the approximation (5.37) of the eigenvalue $\mu(v)$ is valid only near the fixed point. This means that the WKB method, applied after the system-size expansion, fails to accurately approximate the stability well in exactly the same way as the QSS approximation of the full CK equation (see Sec. IV A). We conclude that all of the diffusion approximation techniques fail for the same reason: they cannot estimate the large-deviation behavior of the random process away from the deterministic fixed point.

VI. RESULTS

Thus far, we have developed an approximation of the probability density function for the onset time of an action potential. Building upon earlier studies, which develop analytical and simulation approaches for the case where the stimulus amplitude is above threshold, we now have a quasi-stationary approximation for a below-threshold stimulus amplitude. This allows us to build a complete picture of how stochasticity affects the reliability of neuron's response to stimuli, and for how these results compare to those predicted in the deterministic limit. We have also explored different diffusion approximation techniques and found that each resulted in the same one-dimensional reduced FP equation (4.7), which we now refer to as the diffusion approximation. In this section, we compare the quasi-stationary and diffusion approximations of the MFT, using the theory developed in previous sections along with averaged Monte-Carlo simulations, which are generated with the Gillespie algorithm [27] (see Appendix B for details).

The MFT is computed using the quasi-stationary approximation from Section III and the diffusion approximation (numerical method) from Section IV. Parameter values are listed in Section II, and unless otherwise specified we take $\beta = 0.8\text{s}^{-1}$ so that $\epsilon = 6.9 \times 10^{-3}$. The results of this calculation are shown in Fig. 2.

It is evident that the quasi-stationary approximation is accurate for $I < I_*$ and the diffusion approximation is accurate for $I > I_*$; however, we note that the diffusion approximation is in error by many orders of magnitude as $I \rightarrow 0$. In Fig. 2b we also show the coefficient of variation (CV), defined as the standard deviation over the mean, from the Monte-Carlo simulations, which shows the qualitative transition as the applied current increases past the deterministic threshold ($I_* \approx 40\text{mA}$) from an exponential distribution (CV = 1) to something else for which $\text{CV} < 1$.

To characterize the stochastic nature of the model, one can examine how the fluctuations change as a function of voltage. This quantity is often experimentally accessible and has a convenient theoretical form. When using the diffusion approximation, the random process can be written as a Langevin equation (4.8), in which the noise term contributes fluctuations with magnitude $\sigma(v) = \sqrt{\frac{1}{N}a(v)b(v)^2f(v)^2}$. However, a continuous description of the noise is not valid away from the deterministic fixed point v_0 . To see how this affects the MFT we compute an approximation of stationary distribution, using the FP equation (4.7). We find

$$\hat{u}(v) = \mathcal{N} \exp \left[-\frac{1}{\epsilon} \Phi(v) \right], \quad (6.1)$$

where

$$\Phi(v) = -N \int_{v_*}^v \frac{\nu(v')}{a(v')b(v')^2f(v')^2} dv' \quad (6.2)$$

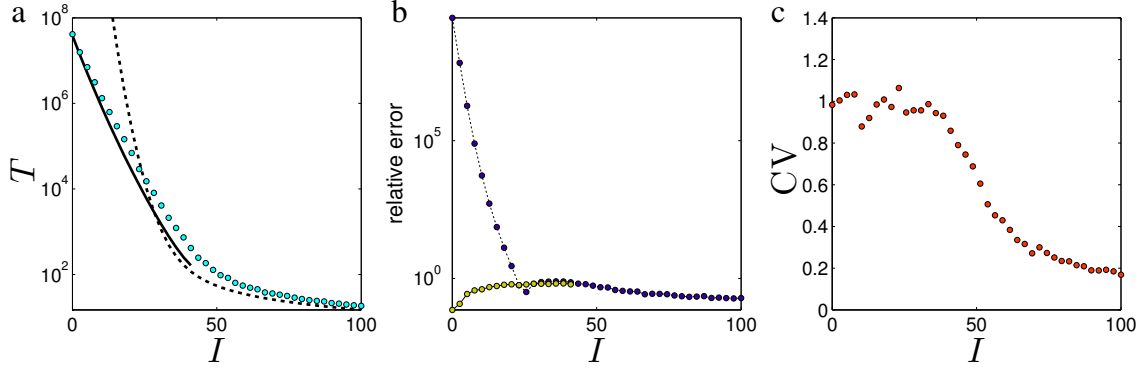


FIG. 2. Mean exit time T (ms) as a function of the applied current I (mA), for $N = 10$. a) The quasi-stationary (solid line) and diffusion (dashed line) approximations are compared to 300 averaged Monte-Carlo simulations (symbols). b) The relative error of each approximation compared to MC simulations. c) CV from the MC simulations.

and \mathcal{N} is a normalization constant. The mean (and deterministic limit) is given by $\nu(v)$ (2.25), and it characterizes the stability properties; that is, the zeros of ν are the deterministic fixed points and the local minima and maxima of $\Phi(v)$. Indeed, Φ can be thought of as a stability landscape, which has multiple wells corresponding to metastable states. Recall that the deterministic system has three fixed points; two are stable, and they are separated by one that is unstable (see Sec. II). We focus on the noise-drive transition from the left stable fixed point v_0 to the unstable fixed point v_* .

The corresponding term in the quasi-stationary approximation is (see Eqn. (3.21))

$$\begin{aligned} \Phi(v) &= - \int_{v_*}^v \mu_1(v') dv' \\ &= -N \int_{v_*}^v \frac{\nu(v') dv'}{b(v')g(v')(f(v') - g(v'))}. \end{aligned} \quad (6.3)$$

In Fig 3, we compare the stability-landscape functions. Both approximations of the stability landscape, Φ , have the same geometry imposed by ν , but the depth of the well is overestimated by the diffusion approximation. Note that the left edge of the well is essentially a vertical wall at $v = v_a \approx -60$ mV, and the right stability well, whose minimum corresponds to the up state, is not shown. Since the MFT is an exponential function of the depth of the well, in general, it is no surprise that the diffusion approximation of the MFT has exponentially-large errors.

The strength-duration curve for a deterministic model is the curve of stimulus amplitudes as a function of stimulus duration that is required to move the potential from rest to threshold. To be specific, for the bistable model (1.1), the strength-duration curve $I = I(T)$ is defined implicitly by

$$T = \int_{v_0}^{v_1} \frac{dv}{a(v)f(v) - g(v; I)}. \quad (6.4)$$

For a stochastic model of action potential initiation, a

natural definition of strength-duration curve is the mean first exit time vs. stimulus amplitude curve, plotted with stimulus amplitude as a function of mean first exit time. Thus, simply reversing the axes in Fig. 2 gives examples of stochastic strength-duration curves. In Fig. 4, additional strength-duration curves are shown for several values of N and ϵ .

For above-threshold amplitudes, the stochastic stimulus durations converge quickly to the deterministic limit as $N \rightarrow \infty$ or as $\epsilon \rightarrow 0$, and the deterministic behavior is qualitatively accurate. For below-threshold amplitudes, the deterministic limit predicts infinite stimulus duration and a zero rate of action potential generation. In contrast, the stochastic model predicts a nonzero rate of action potential generation, which is a behavior that cannot qualitatively be predicted by the deterministic model. While the stochastic behavior converges to the deterministic limit as $N \rightarrow \infty$, the convergence is much slower than predicted by the diffusion approximation. Physically, this suggests that the discreteness of the channel noise makes spontaneous action potentials much more frequent than predicted by the diffusion approximation.

We can also examine the likelihood that a neuron fires an action potential when exposed to a small, constant amplitude stimulus with finite duration t_d . Using the first passage time density $\mathcal{F}(t)$ for action potential initiation, we define the probability of firing an action potential $\text{Prob}\{0 < T < t_d\}$ with

$$\Pi = \int_0^{t_d} \mathcal{F}(t) dt. \quad (6.5)$$

Using the quasi-stationary approximation (3.10), this probability is

$$\Pi \sim 1 - e^{-\lambda_0 t_d}, \quad (6.6)$$

where λ_0 is the firing rate given by (3.72). In Fig. 5 the firing probability is plotted as a function of stimulus amplitude, with a stimulus duration of $t_d = 70$ ms. As expected, close agreement between the quasi-stationary

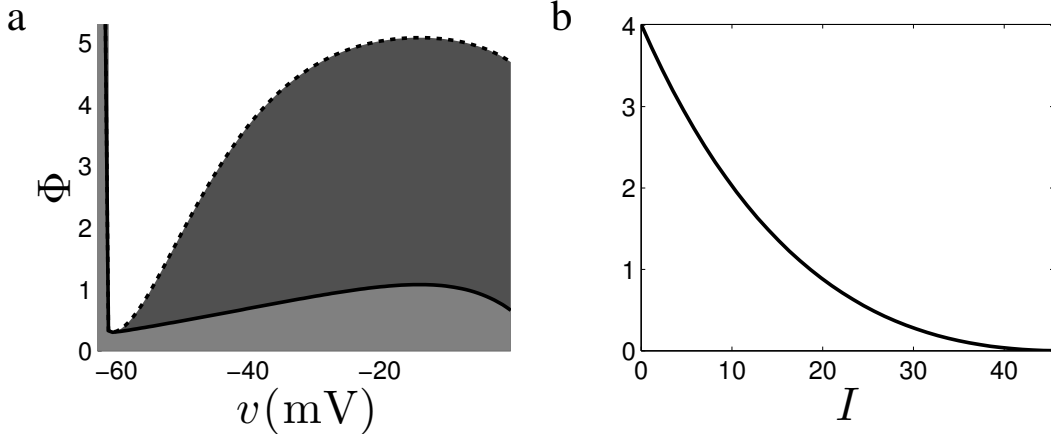


FIG. 3. a) The stability-landscape $\Phi(v)$ from the diffusion (dashed) and quasi-stationary (solid) approximations, with no applied current ($I = 0$). To normalize each curve we have taken $N = 1$, which means that the actual numerical difference in the height of each well should be multiplied by N . For ease of comparison we have added a constant value $C = 0.3 - \Phi(v_0)$ to each version of $\Phi(v)$. b) The difference of the height of each stability well as a function of the applied current I .

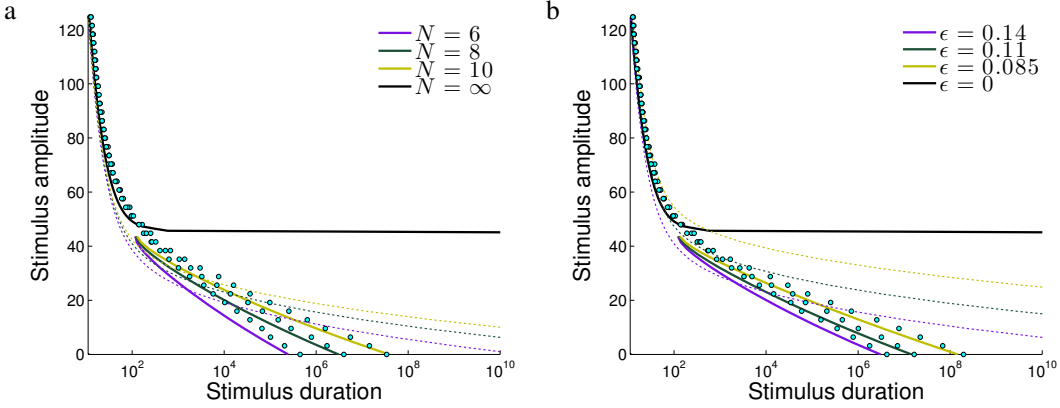


FIG. 4. Strength-duration curves, with the quasi-stationary approximation (solid lines) diffusion approximation (dashed lines) and 10^2 averaged MC simulation (symbols). a) The stimulus amplitude I (mA) as function of the stimulus duration T (ms) for different values of N , the number of channels, with $\beta = 0.8\text{s}^{-1}$. b) Curves for different values of ϵ , which scales the channel switching rate, and $N = 8$. In each, the deterministic strength-duration curve, defined by (6.4), is compared to the stochastic behavior.

approximation and Monte-Carlo simulations is found at low stimulus amplitudes.

VII. DISCUSSION

The goal of extending a successful deterministic model, such as the Hodgkin-Huxley equations, to include stochastic effects is to uncover behavior that the deterministic model cannot predict. In neuroscience, numerous vital functions have been found to depend upon noise, and uncovering the many sources of noise and their effects has been an active area of research in the theoretical community. It has long been known that channel noise can lead to spontaneous action potentials and fuzzy response properties. In this paper, we apply asymptotic

techniques to the problem of estimating the time scale for spontaneous action potential initiation. For applied currents above threshold, the magnitude of fluctuations in the time to fire decreases and the behavior converges to the deterministic limit as the number of channels increases. We can then view the deterministic model, which assumes an infinite number of channels, as an approximation for the true situation, where N is finite. For an applied current below threshold, however, the deterministic model predicts that no action potential is possible, while the stochastic model predicts a nonzero probability of firing. As a result, the deterministic model fails to fully describe the behavior of a single neuron, and this in turn affects any description of how neurons interact in a network.

The message of the paper is twofold. First, we explore

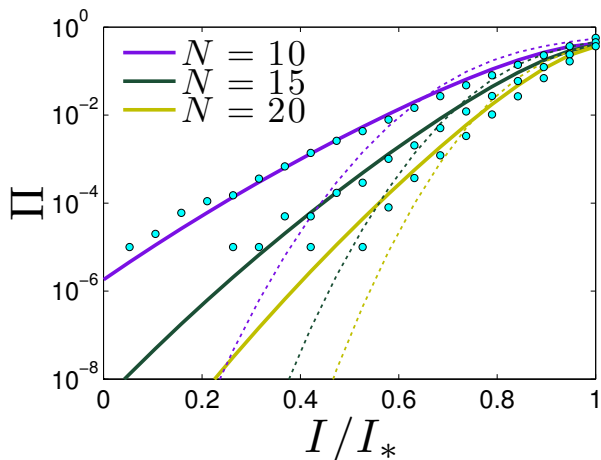


FIG. 5. Firing probability Π as a function of the stimulus amplitude (fraction of threshold) with a stimulus duration of 70ms. The quasi-stationary approximation (solid lines) and the diffusion approximation (dashed lines) are compared to 10^5 averaged Monte Carlo simulations (symbols).

mathematical issues involved in approximating discrete channel noise with a continuous Markov process. This can be done using the QSS reduction or the system-size expansion, the result of which we refer to as the diffusion approximation. For most observable behavior, the diffusion approximation is a powerful and effective tool, but it fails when estimating the timescale for a spontaneous

action potential initiation. Second, we present a quasi-stationary (multiple time scale) analysis, which results in an accurate estimate of this time scale. Our analysis shows that the full, discrete stochastic process must be considered to accurately approximate the latency time for a spontaneous action potential.

Discreteness is an important characteristic of channel noise, and for some behaviors we find that discrete channel noise cannot be approximated by a continuous Markov process. In particular, we find that discreteness affects the strength of random fluctuations away from the deterministic fixed point, making the neuron more responsive to subthreshold stimuli and more likely to generate spontaneous action potentials than an equivalent continuous channel noise. The qualitative picture for the single subunit channel model presented here is not expected to change for a more detailed model of the Sodium channel, which account for the different subunits it contains. Indeed the methods presented here should work equally well for the Hodgkin-Huxley model.

ACKNOWLEDGEMENTS

This publication was based on work supported in part by the National Science Foundation (DMS-0718036) and by Award No KUK-C1-013-4 made by King Abdullah University of Science and Technology (KAUST).

Appendix A

In this appendix, we verify that

$$(\psi_1)_n = \binom{N}{n} (f - g)^{N-n} g^n, \quad (\text{A.1})$$

$$\mu_1 = \frac{N(af - g)}{bg(f - g)}. \quad (\text{A.2})$$

is an eigenpair of the matrix $M = F^{-1}A$, where the matrices A and F are defined by (II) and (2.20). Proceeding by direct calculation, we find that

$$\begin{aligned} v_j(M\psi_1)_j &= (A\psi_1)_j = \sum_{i=j-1}^{j+1} a_{j,i}(\psi_1)_i \\ &= (N - j + 1)\alpha \binom{N}{j-1} h^{N-j+1} g^{j-1} - ((N - j)\alpha + j\beta) \binom{N}{j} h^{N-j} g^j \\ &\quad + (j + 1)\beta \binom{N}{j+1} h^{N-j-1} g^{j+1} \\ &= (N - j + 1)\alpha \binom{N}{j-1} h^{N-j+1} g^{j-1} - (N - j)\alpha \binom{N}{j} h^{N-j} g^j \\ &\quad - j\beta \binom{N}{j} h^{N-j} g^j + (j + 1)\beta \binom{N}{j+1} h^{N-j-1} g^{j+1} \\ &= \alpha h^{N-j} g^{j-1} \left((N - j + 1) \binom{N}{j-1} h - (N - j) \binom{N}{j} g \right) \\ &\quad + \beta h^{N-j-1} g^j \left(-j \binom{N}{j} h + (j + 1) \binom{N}{j+1} g \right) \\ &= (\alpha h^{N-j} g^{j-1} - \beta h^{N-j-1} g^j) \binom{N}{j} N v_j \\ &= (\alpha g^{-1} - \beta h^{-1}) \binom{N}{j} N v_j h^{N-j} g^j \\ &= \frac{\alpha h - \beta g}{hg} N v_j (\psi_1)_j. \end{aligned} \quad (\text{A.3})$$

Appendix B

Monte Carlo simulations are generated using the Gillespie algorithm [4, 7–10, 28–30]. The simulations were coded in C (using the GNU Scientific Library for random number generators) and carried out in MATLAB, using its MEX interface. In between each jump in the number of open channels, the voltage is evolved according to the deterministic dynamics (2.8), which provides the relationship between voltage and time

$$v(t - t_0) = (v(0) - K) \exp \left[\left(g_{\text{eff}} - \frac{S}{N} g_{\text{Na}} \right) t \right] + K \quad (\text{B.1})$$

$$K = \frac{S g_{\text{Na}} v_{\text{Na}} - N g_{\text{eff}} v_{\text{eff}}}{S g_{\text{Na}} - N g_{\text{eff}}}. \quad (\text{B.2})$$

To compute the next jump time, we use the transition rate

$$W(t|S, v(t_0)) = S\beta + (N - s)\alpha(v(t)) = \beta \left(S + (N - S)e^{\frac{2}{v_2}(v(t) - v_1)} \right). \quad (\text{B.3})$$

After integrating the above transition rate, we derive the distribution function for the next jump time:

$$\varphi(t|v(t_0)) = \exp \left[-\beta \left(St + \frac{(N-S)e^{-\frac{2}{v_2}(K+v_1)}}{g_{\text{eff}} - \frac{S}{N}g_{\text{Na}}} Q(t|v(t_0)) \right) \right], \quad (\text{B.4})$$

where

$$Q(t|v(t_0)) = E_i\left(\frac{2}{v_2}(v(t_0) + K) \exp \left[\left(g_{\text{eff}} - \frac{S}{N}g_{\text{Na}} \right) t \right] \right) - E_i\left(\frac{2}{v_2}(v(t_0) + K)\right) \quad (\text{B.5})$$

and E_i is the exponential integral function defined by (3.22). Because the transition rates depend on voltage, and therefore time, the distribution for the next jump time is not explicitly invertible. Let U be a uniform random variable. Then, the next jump time, t , is given implicitly by

$$St + \frac{(N-S)e^{-\frac{2}{v_2}(K+v_1)}}{g_{\text{eff}} - \frac{S}{N}g_{\text{Na}}} Q(t) = -\frac{\log(U)}{\beta}. \quad (\text{B.6})$$

To generate random times, a Newton root finding algorithm is applied to (B.6) until machine precision is reached.

-
- [1] C. H. Luo and Y. Rudy, “A dynamic model of the cardiac ventricular action potential; II: Afterdepolarizations, triggered activity and potentiation,” *Circ. Res.* **74**, 1097–1113 (1994)
 - [2] E. Marban, S. W. Robinson, and W. G. Wier, “Mechanisms of arrhythmogenic delayed and early afterdepolarizations in ferret ventricular muscle,” *J. Clin. Invest.* **78**, 1185–1192 (1986)
 - [3] A. Sherman, J. Rinzel, and J. Keizer, “Emergence of organized bursting in clusters of pancreatic β -cells by channel sharing,” *Biophys. J.* **54**, 411–425 (1988)
 - [4] C. C. Chow and J. A. White, “Spontaneous action potentials due to channel fluctuations,” *Biophys. J.* **71**, 3013–3021 (1996)
 - [5] C. W. Gardiner, *Handbook of stochastic methods for physics, chemistry, and the natural sciences*, Vol. v. 13 (Springer-Verlag, Berlin, 1983) ISBN 0387113576 (U.S.)
 - [6] JA White, JT Rubinstein, and AR Kay, “Channel noise in neurons,” *Trends Neurosci.* **23**, 131–137 (2000)
 - [7] J. R. Clay and L. J. Defelice, “Relationship between membrane excitability and single channel open-close kinetics,” *Biophys. J.* **42**, 151–157 (1983)
 - [8] A. F. Strassberg and L. J. Defelice, “Limitations of the Hodgkin-Huxley formalism - effects of single-channel kinetics on transmembrane voltage dynamics,” *Neural Comp.* **5**, 843–855 (1993)
 - [9] Ronald F. Fox and Yan-nan Lu, “Emergent collective behavior in large numbers of globally coupled independently stochastic ion channels,” *Phys. Rev. E* **49**, 3421–3431 (1994)
 - [10] J. T. Rubinstein, “Threshold fluctuations in an n-Sodium channel model of the node of ranvier,” *Biophys. J.* **68**, 779–785 (1995)
 - [11] Wainrib Gilles, Thieullen Michèle, and Pakdaman Khashayar, “Intrinsic variability of latency to first-spike,” *Biol. Cybern.* **103**, 43–56 (2010)
 - [12] Joshua H. Goldwyn, Nikita S. Imennov, Michael Famulare, and Eric Shea-Brown, “Stochastic differential equation models for ion channel noise in Hodgkin-Huxley neurons,” *Phys. Rev. E* **83**, 041908 (2011)
 - [13] Daniele Linaro, Marco Storace, and Michele Giugliano, “Accurate and fast simulation of channel noise in conductance-based model neurons by diffusion approximation,” *PLoS Comput. Biol.* **7**, e1001102 (2011)
 - [14] Zeev Schuss, *Theory and applications of stochastic processes: an analytical approach*, Applied mathematical sciences, Vol. v. 170 (Springer, New York, 2010) ISBN 9781441916044 (hbk.)
 - [15] Peter Hanggi, Hermann Grabert, Peter Talkner, and Harry Thomas, “Bistable systems: Master equation versus fokker-planck modeling,” *Phys. Rev. A* **29**, 371–378 (1984)
 - [16] M. I. Dykman, Eugenia Mori, John Ross, and P. M. Hunt, “Large fluctuations and optimal paths in chemical kinetics,” *The Journal of Chemical Physics* **100**, 5735–5750 (1994)
 - [17] Charles Doering, Khachik Sargsyan, and Leonard Sander, “Extinction times for birth-death processes: Exact results, continuum asymptotics, and the failure of the Fokker–Planck approximation,” *Multiscale Modeling & Simulation* **3**, 283–299 (2005)
 - [18] Michael J. Ward, “Exponential asymptotics and convection-diffusion-reaction models,” *Bull. Math. Biol.*, 151–184(1998)
 - [19] R Hinch and S. J. Chapman, “Exponentially slow transitions on a Markov chain: the frequency of Calcium sparks,” *Eur. J. Appl. Math.* **16**, 427–446 (2005)
 - [20] Melissa Vellela and Hong Qian, “A quasistationary analysis of a stochastic chemical reaction: Keizer’s paradox,” *Bull. Math. Biol.* **69**, 1727–1746 (2007)
 - [21] Paul C. Bressloff, “Metastable states and quasicycles in a stochastic Wilson-Cowan model of neuronal population dynamics,” *Phys. Rev. E* **82**, 051903 (2010)
 - [22] Jay Newby and Paul C Bressloff, “Local synaptic signaling enhances the stochastic transport of motor-driven cargo in neurons,” *Physical Biology* **7**, 036004 (2010)
 - [23] Jay M. Newby and James P. Keener, “An asymptotic analysis of the spatially-inhomogeneous velocity-jump process,” *in press Multiscale Modeling & Simulation*(2011)

- [24] James P Keener and James Sneyd, *Mathematical physiology*, 2nd ed., Interdisciplinary applied mathematics, Vol. 8 (Springer, New York, NY, 2009) ISBN 9780387094199 (set)
- [25] James P Keener, *Principles of applied mathematics: transformation and approximation* (Perseus Books, Cambridge, Mass., 2000) ISBN 0738201294,
- [26] N. G. van Kampen, *Stochastic processes in physics and chemistry*, 3rd ed., North-Holland personal library (Elsevier, Amsterdam, 2007) ISBN 9780444529657 (pbk.)
- [27] Daniel T. Gillespie, "Exact stochastic simulation of coupled chemical reactions," *J. Phys. Chem.* **81**, 2340–2361 (1977)
- [28] B. Sengupta, S. B. Laughlin, and J. E. Niven, "Comparison of Langevin and Markov channel noise models for neuronal signal generation," *Phys. Rev. E* **81**, 011918 (2010)
- [29] H. Mino, J. T. Rubinstein, and John A White, "Comparison of algorithms for the simulation of action potentials with stochastic Sodium channels," *Ann. Biomed. Eng.* **30**, 578–587 (2002)
- [30] Ian C. Bruce, "Evaluation of stochastic differential equation approximation of ion channel gating models," *Ann. Biomed. Eng.* **37**, 824–838 (2009)

RECENT REPORTS

62/10	Adsorption and desorption dynamics of citric acid anions in soil	Oburger Leitner Jones Zygalakis Schnepf Roose
63/10	A dual porosity model of nutrient uptake by root hairs soil	Zygalakis Kirk Jones Roose Wissuwa
64/10	Hot Charge Pairs and Charge Generation in Donor Acceptor Blends	Kirkpatrick
65/10	Excluded-volume effects in the diffusion of hard spheres	Bruna Chapman
66/10	Dynamics of colloidal particles in ice	Spannuth Mochrie Peppin Wettlaufer
01/11	Improving the efficiency of optical coherence tomography by using the non-ideal behaviour of a polarising beam splitter	Lippok Nielsen Vanholsbeeck
02/11	Self-diffusion in remodelling and growth	Epstein Goriely
03/11	Spontaneous rotational inversion in Phycomyces	Goriely Tabor
04/11	From individual to collective behaviour of coupled velocity jump processes: a locust example	Erban Haskovec
05/11	Solving Eigenvalue problems on curved surfaces using the closest point method	MacDonald Brandman Ruuth
06/11	A numerical methodology for the Painleve equations	Fornberg Weideman
07/11	Strong stability preserving two-step Runge-Kutta methods	Ketcheson Gotlieb MacDonald
08/11	Hysteresis and Post Walrasian Economics	Cross McNamara Kalachev Pokrovskii
09/11	A locally adaptive time-stepping algorithm for petroleum reservoir simulations	McNamara Bowen Dellar
10/11	On the predictions and limitations of the BeckerDoring model for reaction kinetics in micellar surfactant solutions	Griffiths Bain

13/11	Quasi-steady state analysis of two-dimensional random intermittent search processes	Bressloff Newby
14/11	A Constrained Approach to Multiscale Stochastic Simulation of Chemically Reacting Systems	Cotter Zygalakis Kevrekidis Erban
15/11	The Two Regime Method for optimizing stochastic reaction-diffusion simulations	Flegg Chapman Erban
16/11	Recombination via tail states in polythiophene:fullerene solar cells	Kirchartz Pieters Kirkpatrick Rau Nelson
17/11	Energy versus electron transfer in organic solar cells: a comparison of the photophysics of two indenofluorene: fullerene blend films	Soon Clarke Zhang Agostinelli Kirkpatrick Dyer-Smith McCulloch Nelson Durrant
18/11	Asymptotic analysis of a pile-up of edge dislocation	Hall

Copies of these, and any other OCCAM reports can be obtained from:

**Oxford Centre for Collaborative Applied Mathematics
Mathematical Institute
24 - 29 St Giles'
Oxford
OX1 3LB
England
www.maths.ox.ac.uk/occam**